Science Advances
AAAS

advances.sciencemag.org/cgi/content/full/6/34/eabc6378/DC1

Supplementary Materials for

Reengineering biocatalysts: Computational redesign of chondroitinase ABC improves efficacy and stability

Marian H. Hettiaratchi, Matthew J. O'Meara, Teresa R. O'Meara, Andrew J. Pickering, Nitzan Letko-Khait, Molly S. Shoichet*

*Corresponding author. Email: molly.shoichet@utoronto.ca

Published 19 August 2020, *Sci. Adv.* **6**, eabc6378 (2020)
DOI: 10.1126/sciadv.abc6378

The PDF file includes:

Other Supplementary Material for this manuscript includes the following:

(available at advances.sciencemag.org/cgi/content/full/6/34/eabc6378/DC1)

Data files S1 and S2

Table S1. Summary of ChABC stabilization studies. Each row represents a mutant or construct with columns for the study manuscript, sequence mutation from wild type or buffer, substrate, and measured activities where available, including specific activity, V_{max}, K_m, k_{cat}, k_{cat}/K_m, T_m, ΔT_m, and $t_{1/2}$ in normalized units.

Modifications	V_{max} (μM/min)	K_m (μM)	k_{cat} (min^{-1})	k_{cat}/K_m (μM^{-1} min^{-1})	T_m (°C)	ΔT_m (°C)	Half-Life @ 37°C (min)	Study
ChABC-SH3	392	2132, 2175	4894, 4560	2.30, 210	49	-	991	Current Study[a,b]
ChABC-37-SH3	387	2821, 3655	4640, 5759	1.72, 1.58	55	6	6299	
ChABC-55-SH3	64	16180, 4778	802, 2776	0.05, 0.58	57	8	9104	
ChABC-92-SH3	140	2120, 3297	1753, 3722	0.83, 1.14	53	4	4626	
Wild type	0.028	44	5090	116	47	-	2	[43] [a]
With glycerol	0.026	39	4727	121	49	2	30	
With sorbitol	0.023	33	4182	127	52	5	50	
With trehalose	0.025	35	4545	130	54	7	80	
Wild type		42	4980	120	47	-	2	[26] [a]
Q140G		34	5340	156	50	3	5	
Q140A		31	5280	168	53	6	7	
Q140N		50	4800	96	45	-2	1.5	
Wild type	18.7, 5.04	73.1, 8.17	35088, 9396	480, 1150				[44] [a,b]
D433A								
S441A								
N468A								
S474A								
N515A								
N564A								
Y575A								
Y594A								
F609A								
Y623A								
R660A								
N795A	22.5, 4.59	7.25, 13.65	21859, 10008	3015, 733.2				
W818A	19.84, 2.94	16.92, 2.29	15055, 8029	890, 3506				
Wild type	0.029	40.2	5140	128	47	-	3.8	[27] [a]
R692L	0.045	47.3	7000	148	43	-4	3.5	
H700A	0.039	49.2	6877	140	45	-2	3.5	
H700N	0.045	42.2	12,971	307	41	-6	10	

L701T	0.028	56.7	4763	84	57	10	7.5	
Q787A	0.028	40.3	5000	124	51	4	2.5	
H700N, L701T	0.024	48.8	3703	76	63	16	15.8	
R692L, H700A	0.05	27.6	13,210	479	39	-8	2.3	
R692L, Q787A	0.095	28.3	14,875	526	37	-10	2.2	
H700A, Q787A	0.106	29.9	16,562	554	35	-12	1.9	
R692L, H700A, Q787A	0.116	34.3	23,200	676	33	-14	1.5	
Wild type	0.03	41.6	5317	128			3.9	[45] [a]
L679S	0.044	40.6	10682	263			6.6	
L679D	0.029	41.8	5178	124			9.5	
Wild type	0.012	0.52	2223	4254	48	-	8.3	[22] [a]
E131P	0.014	0.692	2072	3427	48	0	9.6	
K132P	0.013	0.84	2028	2414	48	0	5.4	
I134P	0.015	0.75	2438	3223	48	0	4.4	
T136P	0.012	0.48	2034	4172	48	0	6.4	
E138P	0.015	0.76	2238	2920	50	2	18	
Wild type	0.0295	40.8	5090	125			3.8	[46] [a]
M889K	0.0502	27.7	13319	481			9.1	
M889L	0.0296	43.4	5045	116			2.9	
L679D, M889K	0.1055	30	16484	549			11.4	
L679S, M889K	0.0436	41	12262	299			6	
Wild type		0.6624	3433.6	5183.74				[47] [a]
N806Y, Q810Y		0.398	2571.8	6461.83				
N806A, Q810A		0.6099	4395	7206.09				
N806A, Q810Y		0.9494	1860.6	1959.76				
N806Y, Q810A		1.037	2838.6	2737.34				
Wild type	0.01073	662.4	3433.6	5.18374				[48] [a]
I295Y	Inactive	-	-	-				
S581Y	0.01022	614.8	3289.3	5.35024				
G730Y	0.009087	388.1	2368.7	6.10307				
Wild type	0.007321	0.66	3669	5542.2			22.2	[49] [a]
S474H	0.008461	0.77	4231	5436.2			10.6	
H475A	Inactive	-	-	-			-	
Y476H	Inactive	-	-	-			-	

Y476A	Inactive	-	-	-			-	
H475A, Y476H	Inactive	-	-	-			-	
Wild type	0.01	0.57	2426	4257	48	-	8.5	[50] [a]
E138A	0.0136	0.82	2321	2831	48	0	9.9	
E138K	0.015	1.06	1211	1143	48	0	9.9	
E138D	Inactive	-	-	-	42	-6	-	
E138P, Q140A	0.011	0.57	4421	7756	49	1	1.3	
E138P	0.015	0.76	2238	2920	50	2	18	
Wild type					48	-	606	[3] [a]
N1000G					49	1	1218	
Q140G					49	1	444	
T154F					49	1	84	
S431L					50	2	198	
Wild type	0.028	40.4	5224	129	48	-		[51] [a]
Q678E	0.03	42.5	5093	120	47	-1		
Q681E	0.04	51	7005	137	49	1		
Q678E, Q681E	0.046	48.5	7165	148	51	3		

Parameters determined using [a] chondroitin sulfate A or [b] dermatan sulfate as the substrate.

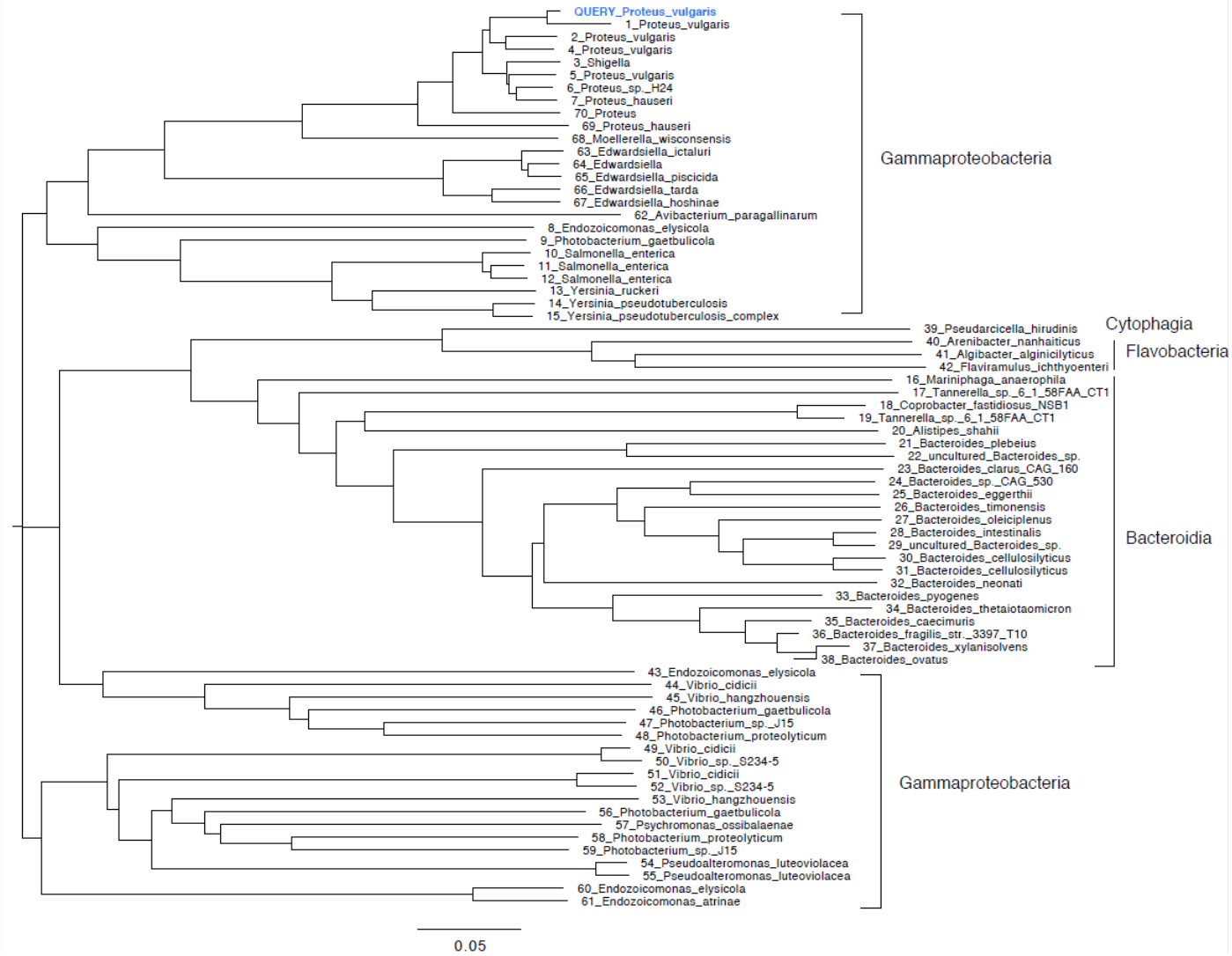

Fig. S 1. Dendrogram for ChABC sequences used to develop consensus design restraints. Protein sequences from the NCBI non-redundant database with BlastP E-value < 1e-4 were aligned using MUSCLE and filtered for the absence of insertions or deletions in DSSP-labeled loops. This process identified 70 sequences. The multiple-sequence alignment is shown as a neighbor-joining tree without distance corrections computed using the clustalo[52] package and plotted using FigTree 1.4.4l, with mid-point rooting labeled with the species and class.[53]

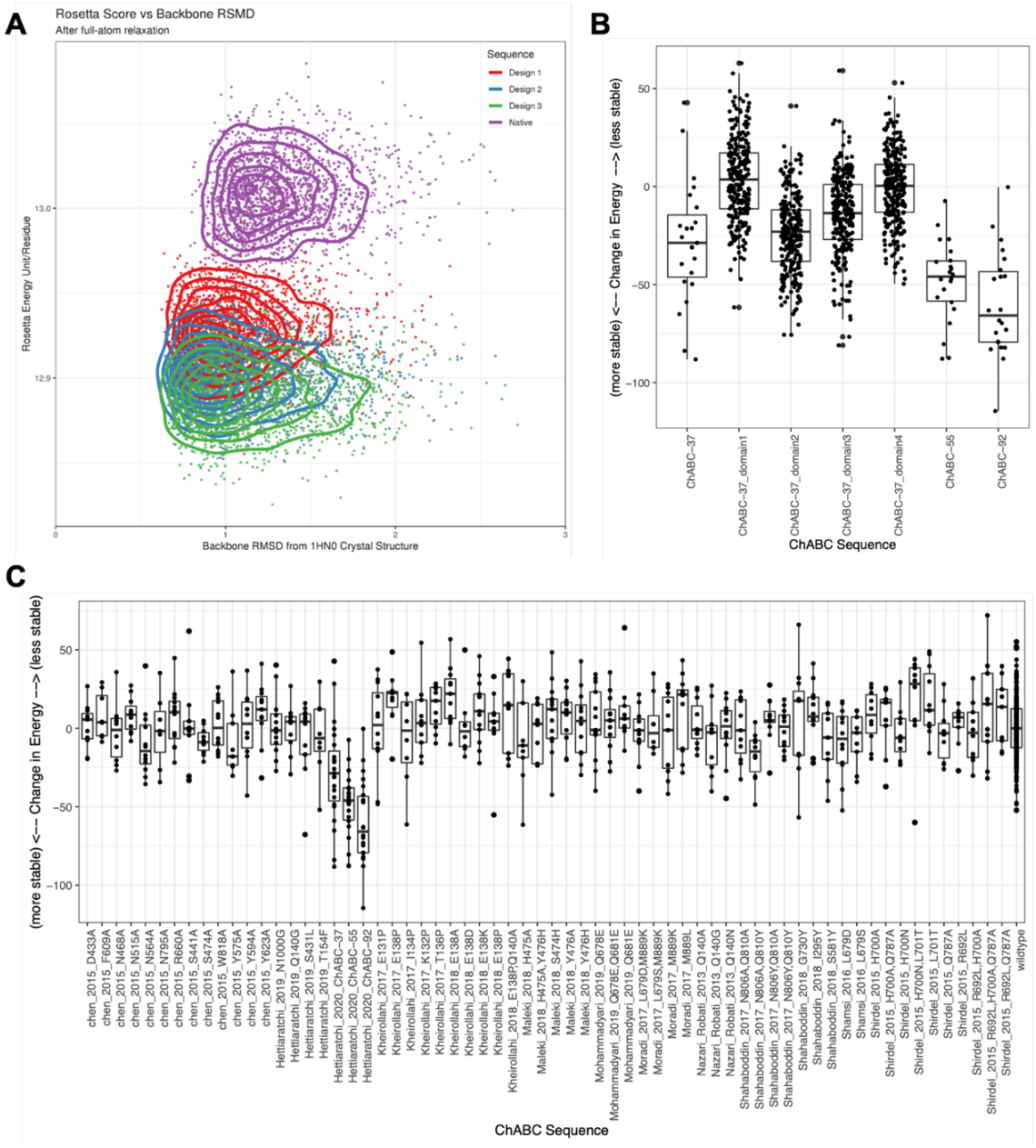

Fig. S2. Global relaxation of wild type ChABC and designed mutants using Rosetta. A) Wild type ChABC and mutants (ChABC-37, ChABC-55, ChABC-92) were relaxed 2000 times each using the FastRelax Rosetta protocol. The result of each relax run is plotted as the predicted energy vs. the backbone root-mean-square deviation (RMSD) from 1HN0. The lower energy designs are predicted to be more stable. B) Wild type ChABC and mutants (ChABC-37, ChABC-55, ChaBC-92) as well as subsets of the ChABC-37 mutations for each domain1-4, having residue ranges 25-242, 243-604, 605-882, 883-1021, and 9, 18, 7, 4 mutations, respectively, were designed with the Rosetta FastDesign protocol. The energy of each design relative to the mean wild type energy is plotted overlaid with a boxplot (ggplot2::boxplot default parameters; mid: median, hinge: 25-75% quantile, and whiskers: 1.5 times inter quantile range of the hinge). C)

Wildtype ChABC mutations, and prior art mutations designed with the Rosetta FastDesign protocol as in Upper Right panel.

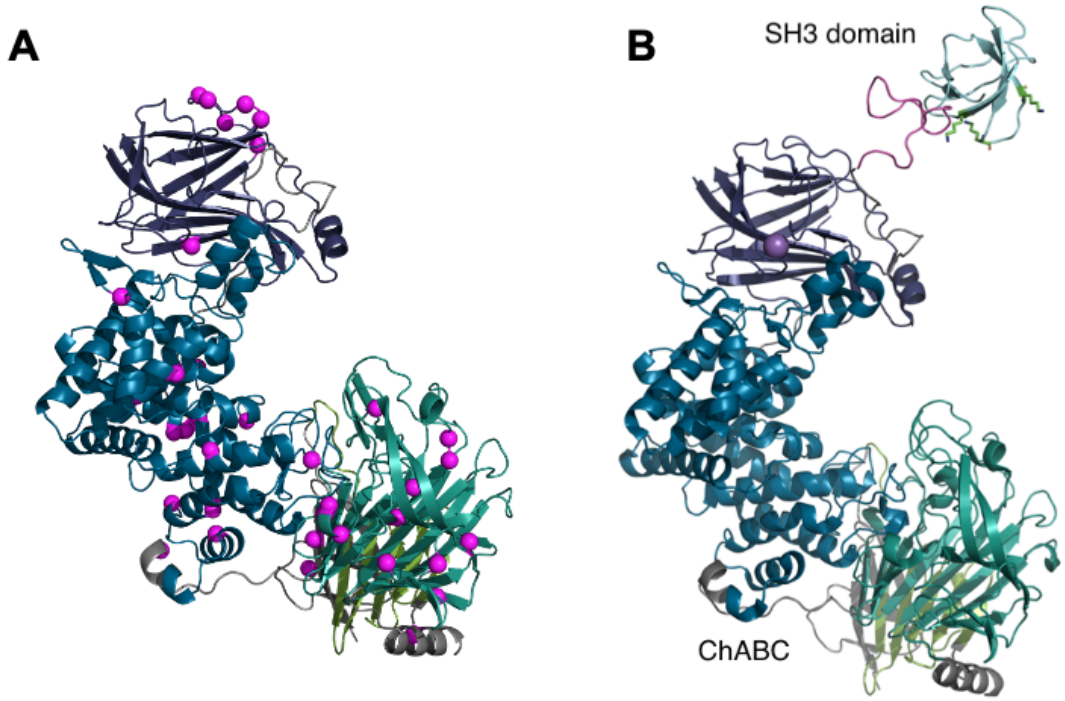

Fig. S3. Additional ChABC and ChABC-SH3 structures. A) Residues mutated in prior to work. 1HN0 with all 46 residues mutated in prior studies listed in Supplemental Table 1. B) Combined ChABC-SH3 model. ChABC (pdb: 1HN0) modeled with N-terminal SH3 domain (pdb: 1JO8) with different colors representing individual domains.

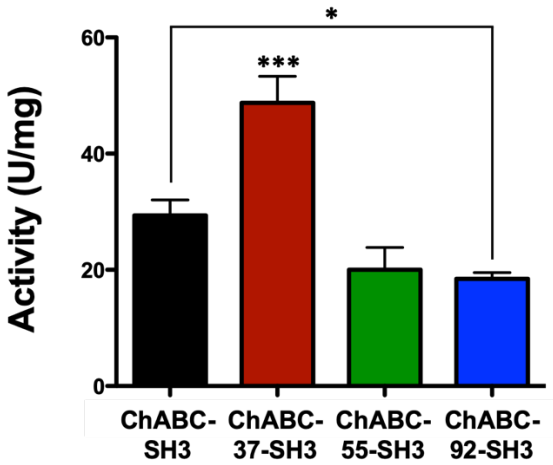

Fig. S4. ChABC-37-SH3 mutant demonstrates higher initial activity for dermatan sulfate compared to ChABC-SH3 and other mutants. (n=3, mean ± SD, *p < 0.05, ***p < 0.001 compared to all other groups)

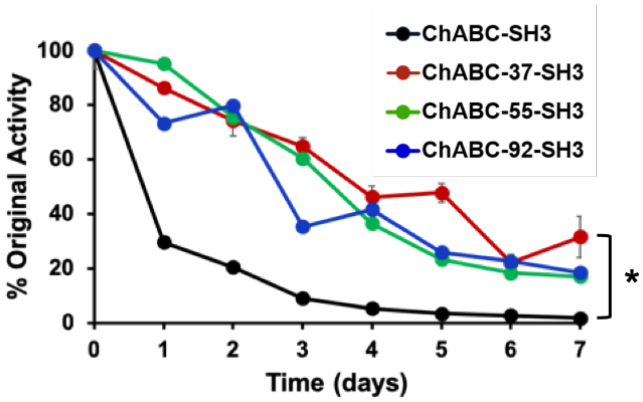

Fig. S5. Activity of wild type ChABC-SH3 and mutants was measured in terms of chondroitin sulfate A degradation and plotted as percentage of original activity. ChABC-SH3 and mutants were incubated at 37 °C in 0.1% BSA in PBS for 7 d (*p<0.05 for ChABC-SH3 vs. ChABC-37-SH3 at all time points) (n=3, mean ± SD).

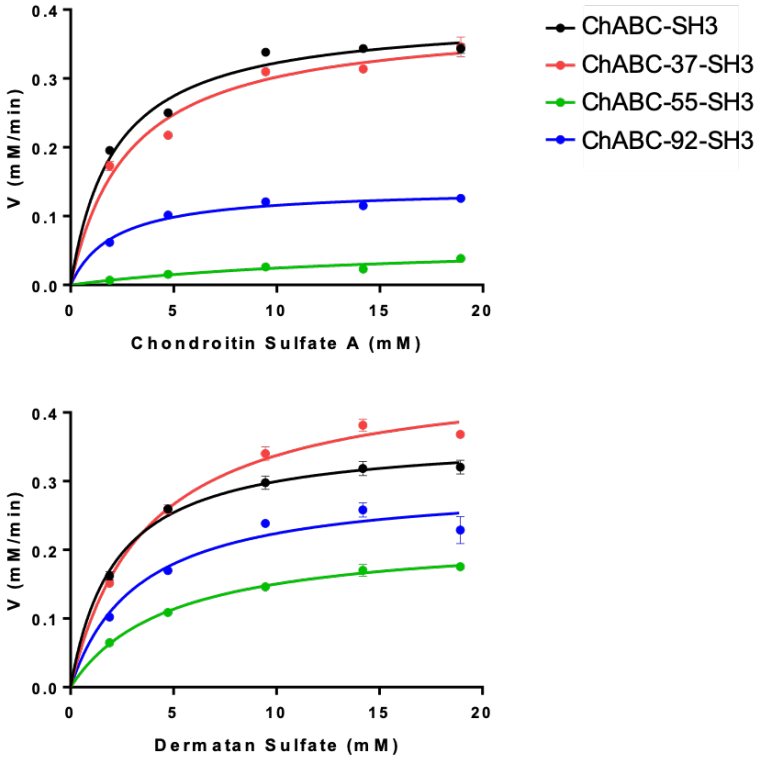

Fig. S6. Michaelis-Menten graphs for the activity of ChABC-SH3 and mutants. Enzymatic activity was measured using two substrates of ChABC: A) chondroitin sulfate A, and B) dermatan sulfate.

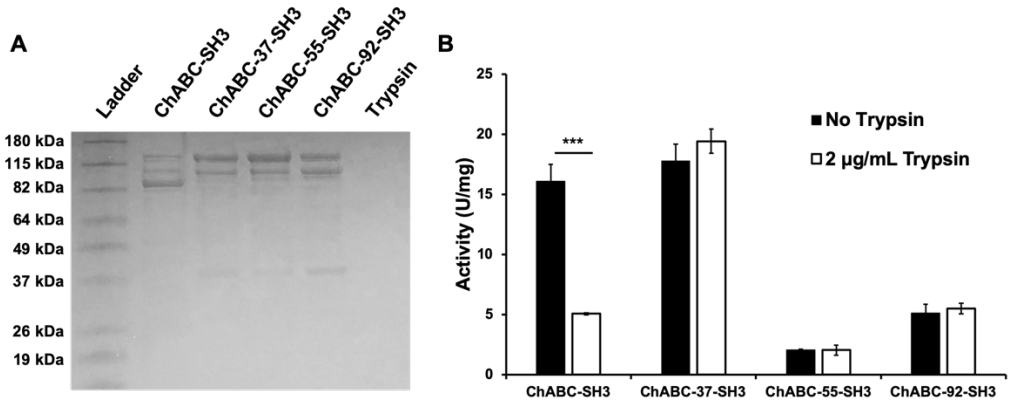

Fig. S7. ChABC-SH3 designs are more resistant to proteolytic degradation than wild type ChABC-SH3. Proteins were incubated in buffer (10 mM $CaCl_2$, 20 mM Tris) with or without 2 µg/mL of trypsin for 45 min at room temperature. A) Gel electrophoresis and Coomassie Brilliant Blue staining of ChABC-SH3 and mutated designs after trypsin treatment. B) Specific activity of wild type ChABC-SH3 and mutants for chondroitin sulfate A with or without trypsin treatment. (***p<0.001 compared to all other groups) (n=3, mean ± SD)

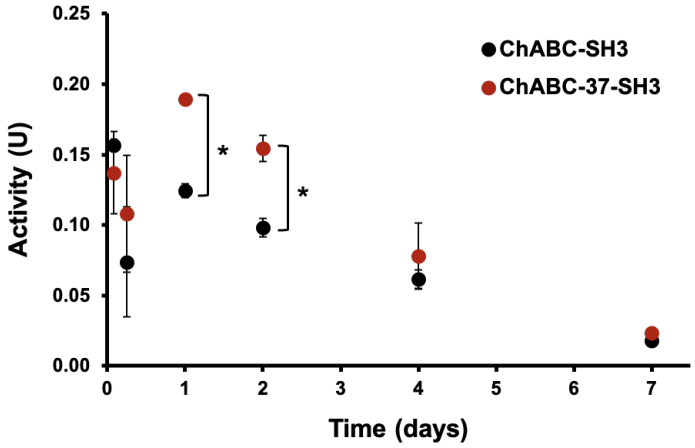

Fig. S8. Activity of ChABC-SH3 and ChABC-37-SH3 released from methylcellulose hydrogels containing affinity binding peptides. 20 µg of either ChABC-SH3 or ChABC-37-SH3 were mixed into 100 µL of methylcellulose hydrogel modified with SH3 binding peptides. The hydrogels released protein into artificial cerebrospinal fluid over 7 d, and the enzymatic activity of the protein was evaluated using chondroitin sulfate A as the substrate. (*p<0.05) (n=3, mean ± SD)

Data file S1. Multiple sequence alignment for extant bacterial ChABC enzyme.

Data file S2. PROSS design output. Including FASTA and PDB files for each predicted design, and a Clustalo alignment of the designs against the wildtype sequence.

REFERENCES AND NOTES

1. A. Hamai, N. Hashimoto, H. Mochizuki, F. Kato, Y. Makiguchi, K. Horie, S. Suzuki, Two distinct chondroitin sulfate ABC lyases: An endoeliminase yielding tetrasaccarides and an exoeliminase preferentially acting on oligosaccharides. *J. Biol. Chem.* **272**, 9123–9130 (1997).
2. D. Shaya, B.-S. Hahn, T. M. Bjerkan, W. S. Kim, N. Y. Park, J.-S. Sim, Y.-S. Kim, M. Cygler, Composite active site of chondroitin lyase ABC accepting both epimers of uronic acid. *Glycobiology* **18**, 270–277 (2008).
3. M. H. Hettiaratchi, M. J. O'Meara, C. J. Teal, S. L. Payne, A. J. Pickering, M. S. Shoichet, Local delivery of stabilized chondroitinase ABC degrades chondroitin sulfate proteoglycans in stroke-injured rat brains. *J. Control. Release* **297**, 14–25 (2019).
4. S. Soleman, P. K. Yip, D. A. Duricki, L. D. F. Moon, Delayed treatment with chondroitinase ABC promotes sensorimotor recovery and plasticity after stroke in aged rats. *Brain* **135**, 1210–1223 (2012).
5. R. Lin, J. C. F. Kwok, D. Crespo, J. W. Fawcett, Chondroitinase ABC has a long-lasting effect on chondroitin sulphate glycosaminoglycan content in the injured rat brain. *J. Neurochem.* **104**, 400–408 (2008).
6. P. M. Warren, S. C. Steiger, T. E. Dick, P. M. MacFarlane, W. J. Alilain, J. Silver, Rapid and robust restoration of breathing long after spinal cord injury. *Nat. Commun.* **9**, 4843 (2018).
7. S. Nori, M. Khazaei, C. S. Ahuja, K. Yokota, J.-E. Ahlfors, Y. Liu, J. Wang, S. Shibata, J. Chio, M. H. Hettiaratchi, T. Führmann, M. S. Shoichet, M. G. Fehlings, Human oligodendrogenic neural progenitor cells delivered with chondroitinase ABC facilitate functional repair of chronic spinal cord injury. *Stem Cell Rep.* **11**, 1433–1448 (2018).
8. E. J. Bradbury, L. D. F. Moon, R. J. Popat, V. R. King, G. S. Bennett, P. N. Patel, J. W. Fawcett, S. B. McMahon, Chondroitinase ABC promotes functional recovery after spinal cord injury. *Nature* **416**, 636–640 (2002).
9. G. García-Alías, S. Barkhuysen, M. Buckle, J. W. Fawcett, Chondroitinase ABC treatment opens a window of opportunity for task-specific rehabilitation. *Nat. Neurosci.* **12**, 1145–1151 (2009).
10. E. S. Rosenzweig, E. A. Salegio, J. J. Liang, J. L. Weber, C. A. Weinholtz, J. H. Brock, R. Moseanko, S. Hawbecker, R. Pender, C. L. Cruzen, Chondroitinase improves

anatomical and functional outcomes after primate spinal cord injury. *Nat. Neurosci.* **22**, 1269–1275 (2019).

11. N. J. Tester, A. H. Plaas, D. R. Howland, Effect of body temperature on chondroitinase ABC's ability to cleave chondroitin sulfate glycosaminoglycans. *J. Neurosci. Res.* **85**, 1110–1118 (2007).
12. N. G. Harris, Y. A. Mironova, D. A. Hovda, R. L. Sutton, Chondroitinase ABC enhances pericontusion axonal sprouting but does not confer robust improvements in behavioral recovery. *J. Neurotrauma* **27**, 1971–1982 (2010).
13. D. M. Fowler, C. L. Araya, S. J. Fleishman, E. H. Kellogg, J. J. Stephany, D. Baker, S. Fields, High-resolution mapping of protein sequence-function relationships. *Nat. Methods* **7**, 741–746 (2010).
14. A. Goldenzweig, M. Goldsmith, S. E. Hill, O. Gertman, P. Laurino, Y. Ashani, O. Dym, T. Unger, S. Albeck, J. Prilusky, R. L. Lieberman, A. Aharoni, I. Silman, J. L. Sussman, D. S. Tawfik, S. J. Fleishman, Automated structure- and sequence-based design of proteins for high bacterial expression and stability. *Mol. Cell* **63**, 337–346 (2016).
15. M. Musil, H. Konegger, J. Hon, D. Bednar, J. Damborsky, Computational design of stable and soluble biocatalysts. *ACS Catal.* 9, 1033–1054 (2019).
16. M. Lehmann, L. Pasamontes, S. F. Lassen, M. Wyss, The consensus concept for thermostability engineering of proteins. *Biochim. Biophys. Acta* **1543**, 408–415 (2000).
17. S. Akanuma, Y. Nakajima, S.-i. Yokobori, M. Kimura, N. Nemoto, T. Mase, K.-i. Miyazono, M. Tanokura, A. Yamagishi, Experimental evidence for the thermophilicity of ancestral life. *Proc. Natl. Acad. Sci. U.S.A.* **110**, 11067–11072 (2013).
18. W. Huang, V. V. Lunin, Y. Li, S. Suzuki, N. Sugiura, H. Miyazono, M. Cygler, Crystal structure of *Proteus vulgaris* chondroitin sulfate ABC lyase I at 1.9Å resolution. *J. Mol. Biol.* **328**, 623–634 (2003).
19. V. Prabhakar, I. Capila, C. J. Bosques, K. Pojasek, R. Sasisekharan, Chondroitinase ABC I from *Proteus vulgaris*: Cloning, recombinant expression and active site identification. *Biochem. J.* **386**, 103–112 (2005).
20. V. Prabhakar, I. Capila, R. Raman, A. Srinivasan, C. J. Bosques, K. Pojasek, M. A. Wrick, R. Sasisekharan, The catalytic machinery of chondroitinase ABC I utilizes a calcium coordination strategy to optimally process dermatan sulfate. *Biochemistry* **45**, 11130–11139 (2006).

21. V. V. Loladze, B. Ibarra-Molero, J. M. Sanchez-Ruiz, G. I. Makhatadze, Engineering a thermostable protein via optimization of charge−charge interactions on the protein surface. *Biochemistry* **38**, 16419–16423 (1999).
22. A. Kheirollahi, K. Khajeh, A. Golestani, Rigidifying flexible sites: An approach to improve stability of chondroitinase ABC I. *Int. J. Biol. Macromol.* **97**, 270–278 (2017).
23. B. W. Matthews, H. Nicholson, W. J. Becktel, Enhanced protein thermostability from site-directed mutations that decrease the entropy of unfolding. *Proc. Natl. Acad. Sci. U.S.A.* **84**, 6663–6667 (1987).
24. H. Zhao, F. H. Arnold, Directed evolution converts subtilisin E into a functional equivalent of thermitase. *Protein Eng. Des. Sel.* **12**, 47–53 (1999).
25. H.-P. Li, Y. Komuta, J. Kimura-Kuroda, T. H. van Kuppevelt, H. Kawano, Roles of chondroitin sulfate and dermatan sulfate in the formation of a lesion scar and axonal regeneration after traumatic injury of the mouse brain. *J. Neurotrauma* **30**, 413–425 (2013).
26. M. Nazari-Robati, K. Khajeh, M. Aminian, N. Mollania, A. Golestani, Enhancement of thermal stability of chondroitinase ABC I by site-directed mutagenesis: An insight from ramachandran plot. *Biochim. Biophys Acta* **1834**, 479–486 (2013).
27. K. Vulic, M. S. Shoichet, Tunable growth factor delivery from injectable hydrogels for tissue engineering. *J. Am. Chem. Soc.* **134**, 882–885 (2012).
28. M. M. Pakulska, C. H. Tator, M. S. Shoichet, Local delivery of chondroitinase ABC with or without stromal cell-derived factor 1α promotes functional repair in the injured rat spinal cord. *Biomaterials* **134**, 13–21 (2017).
29. S. A. Shirdel, K. Khalifeh, A. Golestani, B. Ranjbar, K. Khajeh, Critical role of a loop at C-terminal domain on the conformational stability and catalytic efficiency of chondroitinase ABC I. *Mol. Biotechnol.* **57**, 727–734 (2015).
30. M. Nazari-Robati, A. Golestani, G. Asadikaram, Improvement of proteolytic and oxidative stability of chondroitinase ABC I by cosolvents. *Int. J. Biol. Macromol.* **91**, 812–817 (2016).
31. J. Zuo, D. Neubauer, K. Dyess, T. A. Ferguson, D. Muir, Degradation of chondroitin sulfate proteoglycan enhances the neurite-promoting potential of spinal cord tissue. *Exp. Neurol.* **154**, 654–662 (1998).
32. L. Corvetti, F. Rossi, Degradation of chondroitin sulfate proteoglycans induces sprouting of intact purkinje axons in the cerebellum of the adult rat. *J. Neurosci.* **25**, 7150–7158 (2005).
33. V. Delplace, A. J. Pickering, M. H. Hettiaratchi, S. Zhao, T. Kivijärvi, M. S. Shoichet, Inverse electron-demand diels-alder methylcellulose hydrogels enable the co-delivery of

chondroitinase ABC and neural progenitor cells. *Biomacromolecules* **21**, 2421–2431 (2020).

34. S. El-Gebali, J. Mistry, A. Bateman, S. R. Eddy, A. Luciani, S. C. Potter, M. Qureshi, L. J. Richardson, G. A. Salazar, A. Smart, E. L. L. Sonnhammer, L. Hirsh, L. Paladin, D. Piovesan, S. C. E. Tosatto, R. D. Finn, The pfam protein families database in 2019. *Nucleic Acids Res.* **47** (D1), D427–D432 (2019).
35. S. F. Altschul, T. L. Madden, A. A. Schäffer, J. Zhang, Z. Zhang, W. Miller, D. J. Lipman, Gapped BLAST and PSI-BLAST: A new generation of protein database search programs. *Nucleic Acids Res.* **25**, 3389–3402 (1997).
36. R. C. Edgar, MUSCLE: Multiple sequence alignment with high accuracy and high throughput. *Nucleic Acids Res.* **32**, 1792–1797 (2004).
37. T. A. Whitehead, A. Chevalier, Y. Song, C. Dreyfus, S. J. Fleishman, C. De Mattos, C. A. Myers, H. Kamisetty, P. Blair, I. A. Wilson, D. Baker, Optimization of affinity, specificity and function of designed influenza inhibitors using deep sequencing. *Nat. Biotechnol.* **30**, 543–548 (2012).
38. L. Whitmore, B. A. Wallace, DICHROWEB, an online server for protein secondary structure analyses from circular dichroism spectroscopic data. *Nucleic Acids Res.* **32**, W668–W673 (2004).
39. U. Bodenhofer, E. Bonatesta, C. Horejš-Kainrath, S. Hochreiter, Msa: An R Package for Multiple Sequence Alignment. *Bioinformatics* **31**, 3997–3999 (2015).
40. W. Kabsch, C. Sander, Dictionary of protein secondary structure: Pattern recognition of hydrogen-bonded and geometrical features. *Biopolymers* **22**, 2577–2637 (1983).
41. H. Wickham, *Ggplot2: Elegant Graphics for Data Analysis* (Springer, 2016).
42. L. Schrodinger, The PyMOL Molecular Graphics System. Version 1.3r1 (2010).
43. M. Nazari-Robati, K. Khajeh, M. Aminian, M. Fathi-Roudsari, A. Golestani, Co-solvent mediated thermal stabilization of chondroitinase ABC I form *proteus vulgaris*. *Int. J. Biol. Macromol.* **50**, 487–492 (2012).
44. Z. Chen, Y. Li, Y. Feng, L. Chen, Q. Yuan, Enzyme activity enhancement of chondroitinase ABC I from *Proteus Vulgaris* by site-directed mutagenesis. *RSC Adv.* **5**, 76040–76047 (2015).
45. M. Shamsi, S. A. Shirdel, V. Jafarian, S. S. Jafari, K. Khalifeh, A. Golestani, Optimization of conformational stability and catalytic efficiency in chondroitinase ABC I by protein engineering methods. *Eng. Life Sci.* **16**, 690–696 (2016).

46. K. Moradi, S. A. Shirdel, M. Shamsi, V. Jafarian, K. Khalifeh, Investigating the structural and functional features of representative recombinants of chondroitinase ABC I. *Enzyme Microb. Technol.* **107**, 64–71 (2017).
47. M. E. Shahaboddin, K. Khajeh, M. Maleki, A. Golestani, Improvement of activity and stability of chondroitinase ABC I by introducing an aromatic cluster at the surface of protein. *Enzyme Microb. Technol.* **105**, 38–44 (2017).
48. M. E. Shahaboddin, K. Khajeh, A. Golestani, Establishment of aromatic pairs at the surface of chondroitinase ABC I: The effect on activity and stability. *Appl. Biochem. Biotechnol.* **186**, 358–370 (2018).
49. M. Maleki, K. Khajeh, M. Amanlou, A. Golestani, Role of His-His interaction in Ser^{474}-His^{475}-Tyr^{476} sequence of chondroitinase ABC I in the enzyme activity and stability. *Int. J. Biol. Macromol.* **109**, 941–949 (2018).
50. A. Kheirollahi, K. Khajeh, A. Golestani, Investigating the role of loop 131–140 in activity and thermal stability of chondroitinase ABC I. *Int. J. Biol. Macromol.* **116**, 811–816 (2018).
51. H. Mohammadyari, S. A. Shirdel, V. Jafarian, K. Khalifeh, Designing and construction of novel variants of chondroitinase ABC I to reduce aggregation rate. *Arch. Biochem. Biophys.* **668**, 46–53 (2019).
52. F. Madeira, Y. M. Park, J. Lee, N. Buso, T. Gur, N. Madhusoodanan, P. Basutkar, A. R. N. Tivey, S. C. Potter, R. D. Finn, R. Lopez, The EMBL-EBI search and sequence analysis tools APIs in 2019. *Nucleic Acids Res.*, **47** (W1), W636–W641 (2019).
53. A. Rambaut, FigTree v1. 4.2, A Graphical Viewer of Phylogenetic Trees. (2018).